

Volume of B_2O_3 at the glass transition

R. Brüning and M. Sutton

*Centre for the Physics of Materials, Department of Physics, McGill University, Rutherford Physics Building,
3600 University Street, Montréal, Québec, Canada H3A 2T8*

(Received 28 September 1993)

The glass transition of B_2O_3 is characterized on time scales ranging from about 10^3 to 10^6 s by continuous measurements of the volume expansion upon cooling and heating. The data show a linear relationship between the glass transition temperature and the logarithm of the heating or cooling rate. The hysteresis of the volume at the glass transition becomes narrower at lower rates. The data are compared to two models for the nonequilibrium kinetics at the glass transition.

INTRODUCTION

At the glass transition a supercooled liquid leaves a metastable equilibrium and forms a nonequilibrium glassy structure. Chemically and structurally very different systems such as oxides, organic compounds, polymers or metal alloys follow strikingly similar kinetics when they form glasses. Thus studying the kinetics may provide insight into the nature of the glass transition, yet the measurement of the kinetics over a sufficient range of times is difficult, since the time scale over which observed properties change varies exponentially with temperature. For this reason techniques are needed which allow one to extend the time scale of measurements. One approach is to anneal samples and to characterize them afterwards. For example, after cooling samples continuously through the glass transition one can measure their density¹ or the specific heat upon reheating.² Similar measurements were made by Boehm, Ingram, and Angell on samples that were annealed isothermally for several years.³ Since the glass transition is not observed directly, data obtained by these techniques require some amount of interpretation. The most common technique to measure the glass transition directly is to scan the temperature at a constant rate φ , in a differential scanning calorimeter (DSC).^{1,2,4} This provides data of high precision for the changes of the specific heat C_p . However the DSC heat-flow signal decreases with the rate of the temperature change, and the range over which kinetic data can be obtained is restricted by the signal-to-noise ratio. Furthermore, due to problems in subtracting background signals, the less well defined signature of the glass transition upon cooling may only be measured in the most favorable cases. Recently relaxation calorimetry has been used to obtain data on cooling, but this method does not allow cooling at a constant rate.⁵ Measurement of the volume avoids the most important problems associated with calorimetric measurements as the signal-to-noise ratio does not depend on the heating rate.

Here continuous measurements of the volume of B_2O_3 are reported. B_2O_3 forms a network glass and has been studied extensively. The temperature dependence of the viscosity, the enthalpy and the volume at the glass transition are well known,^{2,6} and the microscopic structural

changes have been identified by Raman scattering⁷ and neutron diffraction.⁸ The system was cooled from metastable equilibrium through the glass transition at the rate $-\varphi$, and then heated at the rate φ until it once again reaches metastable equilibrium. Together with previously published calorimetry data, the data for B_2O_3 span the range from 0.001 to 80 K/min. For comparison, the 5-m-diam mirror of the Palomar telescope was cooled at a rate of 0.0006 K/min after casting.⁹ It is not clear *a priori* whether the enthalpy and the volume changes will follow the same kinetics at the glass transition, and discrepancies between the relaxation of different properties have been reported.² However the comparison of the present results with the DSC data indicate no measurable difference in the kinetics, as one should expect if the same microscopic processes cause the changes of the specific heat C_p , and the volume expansion coefficient α , at the glass transition.

Several kinetic equations have been suggested to describe the nonequilibrium kinetics in systems near the glass transition. Most employ modified Arrhenius kinetics such that the time constant τ has the basic form $\tau \propto \exp(E_a/kT)$, where E_a is the height of a free-energy barrier and k is Boltzmann's constant.¹⁰ In some cases the more general Vogel-Fulcher form for the time constant, $\tau \propto \exp[B/(T-T_0)]$, was found to be more accurate.^{4,5,11,12} This is an interesting behavior because the divergence implies the transition to an "ideal glass" at T_0 .¹¹ The present data are compared to two models which provide specific kinetic equations. The "delayed response model," also referred to as the "four parameter model," was suggested by Moynihan and co-workers.^{2,10} The model is based on Arrhenius kinetics and predicts the state of the glass forming system for an arbitrary thermal history based on a set of four parameters and it was first applied to specific-heat measurements of the glass transition in B_2O_3 . The model assumes that a single variable, the fictive temperature T_f is sufficient to describe the nonequilibrium state of the system at constant pressure. Following the definition of the fictive temperature employed by Moynihan and co-workers,^{2,13} T_f for the system at a temperature T is given by

$$\int_{T^*}^{T_f} (\alpha_L - \alpha_G) dT' = \int_{T^*}^T (\alpha - \alpha_G) dT', \quad (1)$$

where α is the thermal-expansion coefficient, α_L and α_G are the (extrapolated) volume expansion coefficients for the liquid and the glass, and T^* is an arbitrary reference temperature taken to be above the glass transition region where $\alpha = \alpha_L$ and the system is in equilibrium. The model assumes that T_f follows a change of temperature with a delayed, nonexponential response. The response function depends on a characteristic delay time τ and it is approximated with stretched exponential form with a power β . Integrating these delayed responses gives

$$T_f(T) = T^* + \int_{T^*}^T \left\{ 1 - \exp \left[- \left(\int_{T^*}^{T'} \frac{dT''}{\tau \varphi(T'')} \right)^\beta \right] \right\} dT' . \quad (2)$$

The time constant τ depends both on the temperature T and the state of the system through T_f . It is approximated by

$$\tau(T) = A \exp \{ (x E_a / kT) + [(1-x) E_a / kT_f(T)] \} , \quad (3)$$

$$T_f(T) = T^* + \int_{T^*}^T \exp \left[\frac{-E_a}{kT'} \right] \left\{ \exp \left[\frac{-B}{\tilde{T} - T_0} \right] - \exp \left[\frac{-B}{T_f(T') - T_0} \right] \right\} \frac{[T_f(T') - T_0]^2}{AB\varphi} dT' , \quad (4)$$

where $\tilde{T} = \max(T', T_{0+})$ and A , E_a , B , and T_0 are the parameters of the model. In addition the model is constrained, since T_0 and B are expected to be related to the equilibrium viscosity by $\eta_{eq} \propto \exp[B/(T - T_0)]$. Both models are tested against the present data. A least-squares fitting procedure is used to find the best set of parameters to fit the data for each model.

EXPERIMENTAL METHOD

A dilatometer was built to measure the volume expansion of B₂O₃. The dilatometer consists of a sample cell filled with B₂O₃ and mercury, and the thermal expansion is measured by observing the change of the mercury level in a capillary tube connected to the sample cell. A schematic drawing of the apparatus is shown in Fig. 1. The design and operation followed mostly the description by Bekkedahl.¹⁷ A cylindrical stainless steel sample cell with a volume of 9.4 cm³ is closed at the bottom by a lid with a steel-steel compression seal. A steel capillary tube is attached to the lid. The sample cell was inverted and filled in several steps with 16.0 g B₂O₃ (99.999%, Aldrich Chemical Co.). After some B₂O₃ was added, the cell was heated under vacuum to 1250 K for several hours to obtain a sample with a low water content and which is free of bubbles.^{7,18} This was repeated until the cell was completely filled. Then the sample cell was inverted again and placed inside the furnace of the dilatometer for the measurements. An aluminum jacket between the sample cell and the heating wire helped to reduce temperature gradients. Outside the furnace the steel capillary was then connected to a U-shaped glass capillary tube with 2.0 mm inside diameter. The capillary and the sample cell were evacuated and filled with mercury¹⁷ to a level

where E_a is the characteristic activation energy, k is Boltzmann's constant, and A is a time prefactor. The coefficient x determines to which extent the time constant is determined by the temperature and the state of the system. In Eq. (2), φ is not necessarily constant. In the current experiment, φ is first negative upon cooling then positive upon heating.

A "defect concentration model," suggested by Sietsma and co-workers,¹⁴⁻¹⁶ has been developed to describe the glass transition in metallic glasses. This model is an adaptation of the free volume model and allows one to calculate the viscosity, the elastic properties, the enthalpy, and the volume of glasses for any thermal history. The kinetics are expressed in terms of the concentration of defects, which the model relates to the free volume. The state of the system is given by the free volume, which may be expressed in terms of a fictive temperature using Eq. (1). Unlike the delayed response model, the fictive temperature must always remain above a temperature T_0 . The evolution of T_f is given by

about 150 mm above the bottom of the sample cell. During the measurement, the level in the glass capillary is monitored by an infrared emitter and receptor diode pair, which is maintained at the height of the meniscus of the mercury column by a feedback controlled servo system. The voltage output of the servo circuit, which corre-

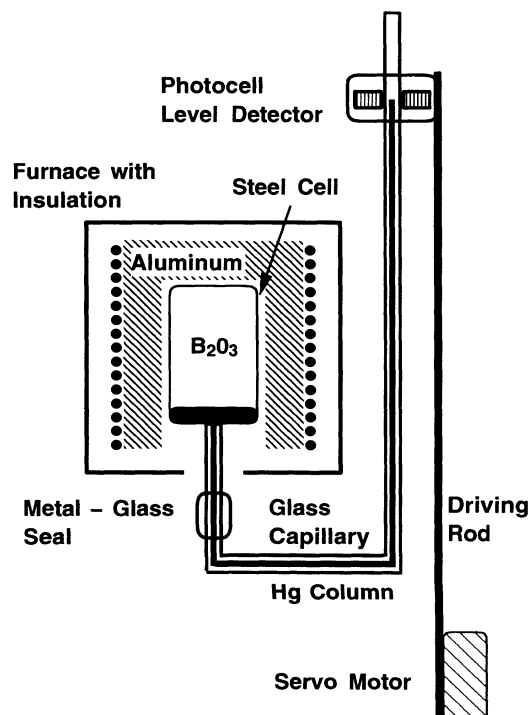


FIG. 1. Schematic diagram of the experimental apparatus to measure the volume expansion of B₂O₃ through the glass transition.

sponds to the height of the meniscus, is recorded by a computer. The temperature is measured by two thermocouples, which are placed at the side and the top of the sample cell. The computer controls a heater and records the temperature. The sample is cooled from a temperature above the glass transition at a rate of $-\varphi$ to well below the glass transition regime and is reheated to above the glass transition at the same rate φ , for φ ranging from 0.001 to 2 K/min. The raw data were corrected for the thermal expansion of the stainless steel cell, $5.43 \times 10^{-5} \text{ K}^{-1}$.¹⁹

The specific volume of B_2O_3 for heating and cooling at 1, 0.5, and 0.001 K/min is shown in Fig. 2 as a function of temperature. The data are consistent with the results obtained by Macedo, Capps, and Litovitz.¹⁸ The supercooled liquid state is characterized by a steep slope, i.e., a high volume expansion coefficient. The formation of the glass appears as the transition to a more shallow slope. The temperature where the volume deviates from the steep equilibrium liquid curve decreases with the cooling rate, and therefore cooling at a slower rate results in a glass with a higher density. The change in the height of the mercury column is about 1.1 mm/K above the glass transition and 0.1 mm/K below the glass transition. The signal was differentiated with respect to temperature to obtain the volume expansion coefficient. Figure 3 shows the thermal-expansion coefficient, smoothed over 2 K, as a function of temperature for different rates. The noise is mostly due to the irregular changes of the mercury column of the dilatometer. The deviation between the temperature setpoint and the two measured temperatures is always less than 1.5 K, and usually well below 1 K. However a temperature gradient ΔT exists between the thermocouples outside the sample cell and the sample. From the information of both the heating and the cooling curves a self-consistent correction for the temperature lag of the apparatus is possible. The effect of the lag may be

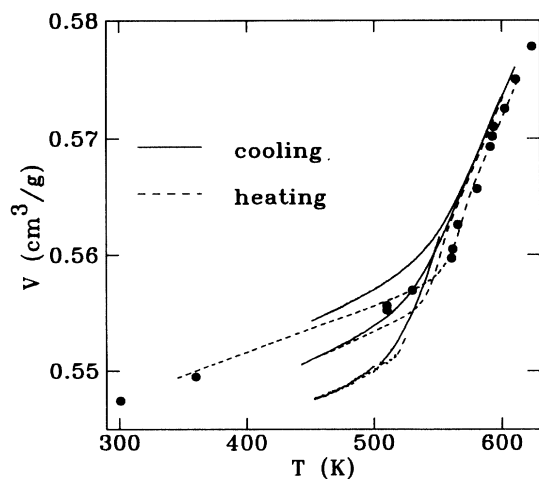


FIG. 2. Specific volume of B_2O_3 around the glass transition measured at the rates 1, 0.05, and 0.001 K/min (top to bottom). In all experiments the glass was first cooled from above T_G to below T_G , and then reheated with the same rate. The points represent pycnometric data from Ref. 18.

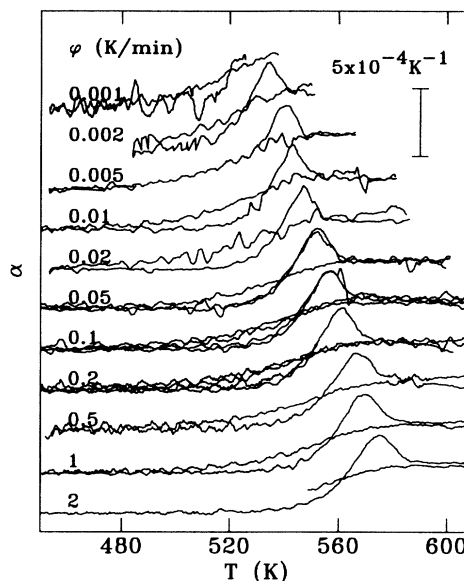


FIG. 3. Volume expansion coefficient of B_2O_3 at the glass transition upon cooling and heating at different rates φ . The smooth curves are the data obtained on cooling, and the overshoot occurs during heating as the sample regains equilibrium. All data were smoothed over an interval of 2 K. Data from repeated measurements demonstrate the reproducibility of the results.

approximately canceled by correcting the measured temperature upon cooling by ΔT and the temperature for the data on heating by $-\Delta T$. ΔT was determined by introducing this correction as an additional parameter in the fitting of the experimental data to the delayed response model. This procedure visibly improved the fits to the data at high heating and cooling rates, and the fits for traces at different rates φ gave consistently $\Delta T/\varphi = (2.63 \pm 0.05) \text{ min}$. (For a DSC one typically finds $\Delta T/\varphi = 0.10 \text{ min}$.) Subsequently, ΔT was fixed to these values and all data are presented with the temperatures corrected. The further results of the fitting procedure are discussed below.

RESULTS AND DISCUSSION

Figure 3 shows the hysteresis between the heating and cooling curves caused by the dependence of the state of the system on the thermal history. The point where the glass is formed depends on the rate of cooling, and the specific volume of the glass decreases with decreasing cooling rate. Here the difference in volume after cooling at the fastest and the slowest rates is about 1.3% (Fig. 2). α_l is a function of temperature which for the relevant temperature range may be approximated by $\alpha_l(T) = \alpha_L^0 + \alpha_L^1 T$, with $\alpha_L^0 = 12.1 \times 10^{-4} \text{ K}^{-1}$ and $\alpha_L^1 = -0.013 \times 10^{-4} \text{ K}^{-2}$, while $\alpha_G = 1.0 \times 10^{-4} \text{ K}^{-1}$ is temperature independent. The numerical values are based on the results in Ref. 18. This simplifies Eq. (1) to

$$\alpha(T) = \alpha_G + \frac{dT_f(T)}{dT} [\alpha_L^0 + \alpha_L^1 T_f(T) - \alpha_G]. \quad (5)$$

The minimum of the fictive temperature reached by the sample upon cooling at a specific rate, $\min(T_f)$, is perhaps the best defined measure of the glass transition temperature, since it does not depend on the shape of the hysteresis loop. As will be discussed below the delayed response parameter model reproduces the data very well. To achieve greater precision $\min(T_f)$ was calculated from the fit of the delayed response model to the data rather than directly from the data. Figure 4 shows the values of the glass transition temperature from the present data and previously reported results.^{2,4} For the whole range of cooling and heating ranges $\min(T_f)$ depends linearly on $\log_{10}(\varphi)$, and the three sets of data are consistent with a single slope. The offsets between the different sets of data are mostly caused by varying amounts of water dissolved in the B₂O₃. Dissolved water decreases the glass transition temperature,⁴ which most likely reflects that the network glass relaxes faster with bonds broken due to hydrogenation and thus evolves further for a given time. From the present results it is obvious that the calorimetric data for B₂O₃ at rates faster than 50 K/min in Ref. 4, which are not included in Fig. 4, seriously overestimated the glass transition temperature. This was most likely caused by thermal gradients within the sample which were not taken into account by calibrating the DSC with metal melting point standards with high thermal conductivity. Measuring the glass transition upon cooling and heating allows us to correct the present data for temperature gradients self-consistently.

In Fig. 5 the data are shown with the temperature normalized with $\min(T_f)$. The lines are guides to the eye which point out characteristic points on the hysteresis loops. They show that the glass transition becomes sharper as the measurement is made on a longer time

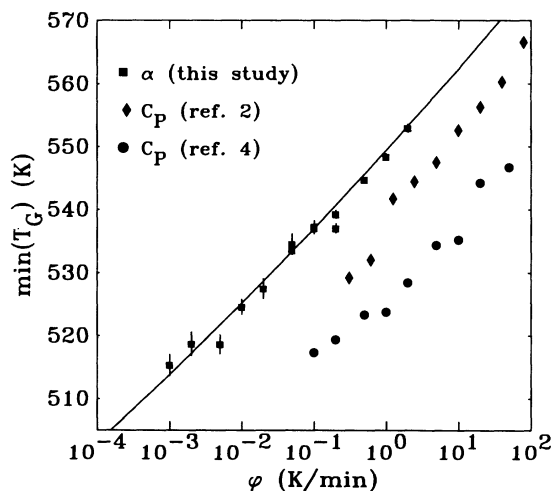


FIG. 4. Glass transition temperature of B₂O₃ obtained from volume expansion and specific-heat measurements. For the data from Ref. 2 and the present results T_G was taken as $\min(T_f)$, while for the other data T_G was defined as the onset of the glass transition (Ref. 4). The line is the best fit of the present data to Eq. (6).

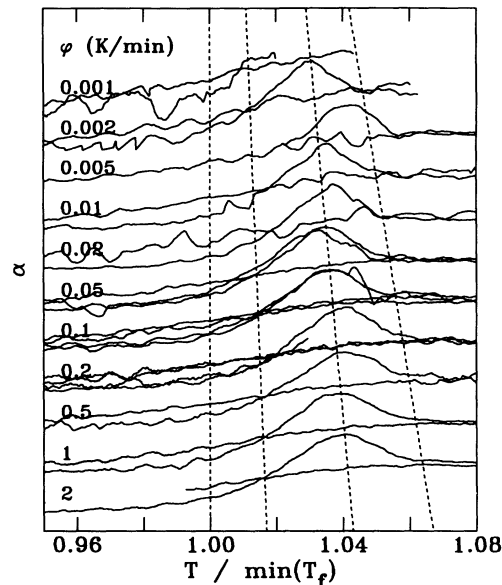


FIG. 5. Volume expansion coefficient at the glass transition measured of different rates with the temperatures scaled with $\min(T_f)$. The dashed lines approximate the points where $T = T_f$ the thermal-expansion coefficients upon cooling and heating are equal, the temperature of the maximum thermal-expansion coefficient upon heating and the temperature where the system deviates from metastable equilibrium (left to right).

scale. The sharpening is about 10% for every decade decrease in the heating rate. As a consequence the curves cannot be described by a single temperature-time scaling relationship $\tau \propto \exp(E_A/kT)$. Instead each feature of the curves would give a different value of E_A .

The delayed response model and the defect concentration model both allow a fit to the shape of the volume expansion curves. Figure 6 shows the best fits given by both equations to the data obtained at $\varphi = 0.1$ K/min.

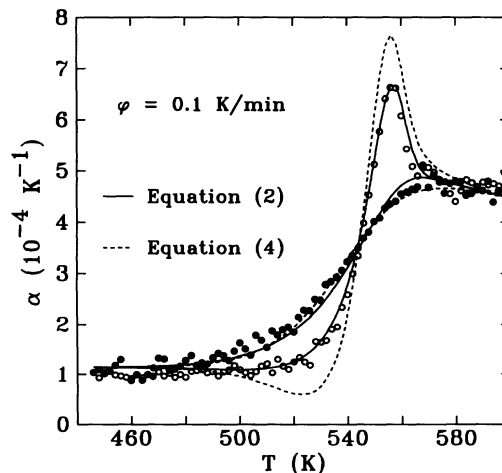


FIG. 6. Volume expansion coefficient for $\varphi = 0.1$ K/min and best fit of Eqs. (2) and (4) to the data.

For Eq. (2) the parameters A , E_a , x , and β were varied, while for Eq. (4) the parameters A , E_a , and T_0 were fit. The fit of the data to the delayed response model is excellent, and the choice of parameters are discussed below in detail. The fit of the data to the defect concentration model, Eq. (4), also reproduces the data quite well. The parameter B was set to 1825 K, which is the value found by Macedo and Napolitano for a fit of the viscosity data for B_2O_3 to a Vogel-Fulcher form.⁶ The parameters which gave the best fit were $T_0=335$ K, $E_a=1.8$ eV, and $A=2\times 10^{-17}$ s. Varying B did not improve the fit significantly. The value obtained for T_0 is fairly consistent with $T_0=411$ K found by Macedo and Napolitano. For an activated process in a solid one expects $1\text{ eV} < E_a < 1.5\text{ eV}$ and $A < 10^{-13}$ s. The values found for E_a and A are much closer to these values compared to the delayed response model. Although Eq. (4) does not produce the best fit to the data, the fitted parameters suggest that it describes two aspects: the relationship between the equilibrium viscosity and the equilibrium defect concentration, and the importance that the latter has in determining the kinetics.

The delayed response model [Eq. (2)] assumes that a single set of parameters is sufficient to describe the data for all cooling and heating rates. To test this assumption, the parameters of the delayed response model were adjusted to give the best fit to the data for each rate φ . Figures 6 and 7 show that the fits with four varying parameters reproduce the shape of the experimental traces very well. Traces calculated for a fixed set of parameters deviate in a systematic way from the data (Fig. 7). The figure shows that the delayed response model fails to describe the observed narrowing of the hysteresis loop with decreasing φ . [For fixed parameters the defect concentration model predicts a much smaller shift of T_f with $\log_{10}(\varphi)$ than observed such that, compared to the delayed response model, the discrepancy between the calculated curves and the data is worse.] The values of the pa-

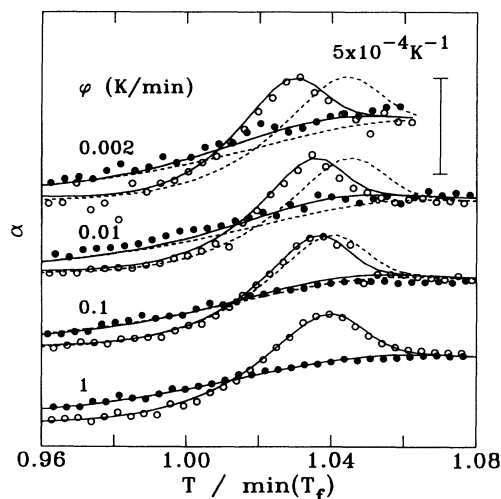


FIG. 7. Data (points) with the best fits to the delayed response model (solid line). The broken lines show the calculated curves for the fitted parameters obtained for $\varphi=1$ K/min.

rameters obtained for the delayed response model are shown in Fig. 8 together with the values found by DeBolt *et al.*² Figure 8 shows that in spite of the systematic trend in the fits to the data, the variation of the fitted parameters is not very large. The parameters E_a and A are very strongly correlated. These are mostly determined by the glass transition temperature and to a lesser degree by the width of the hysteresis loop. Although the values of $\min(T_f)$ were calculated from the fitted parameters with large variations in E_a and A , most of these variations cancel and only small uncertainties in the value of $\min(T_f)$ remain. Equation (3) is based on the assumption of an Arrhenius process. Upon continuous heating an Arrhenius process of order one has the highest rate at a temperature \hat{T} , given by

$$k\hat{T}^2/\varphi = AE_a \exp(E_a/k\hat{T}). \quad (6)$$

This relationship is valid as a good approximation, and allows an independent calculation of E_a and A . The line in Fig. 4 is the best fit of the data to Eq. 6 with $\hat{T}=\min T(T_f)$. The corresponding values of E_a , A and their standard errors, shown by the broken lines in Fig. 8, agree with the average values of the fitted parameters. The parameters x and β control the difference between the cooling trace and the heating trace and the height of the overshoot upon heating, and their effect on T_f and the width of the hysteresis is small. The calorimetric and dilatometric measurements give fitted parameters which agree quite well (Fig. 8), and the heating rate dependence of the glass temperature is also consistent for the two

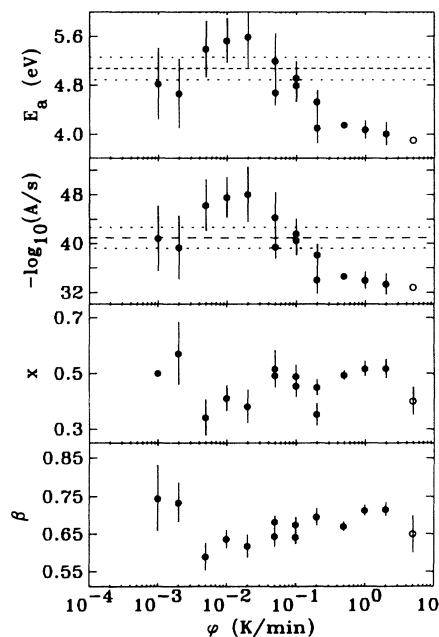


FIG. 8. Parameters of the fit of the delayed response model to the data at different heating rates (full circles). Values of the constant parameters in Ref. 2 are shown at the average of the rates used in these experiments (open circles). The broken lines indicate the values for E_a and A corresponding to the fit of the data to Eq. (6) and the standard error. For $\varphi=0.001$ K/min the parameter x was set to 0.5.

types of experiments (Fig. 4). This indicates that the same kinetics govern the changes of the enthalpy and the volume at the glass transition, and it is very likely that identical microscopic processes cause both macroscopic changes. Based on Raman scattering and neutron-diffraction results it has been proposed that the number of boroxol rings in the melt increases with decreasing temperature.^{7,8} At T_G the proportion of rings in the structure is estimated to be 60%, with the rest of the molecules arranged in chains.⁷ Following the same estimate, the difference between the number of boroxol rings in the glass formed upon cooling at 2 K/min and the glass formed at 0.001 K/min would only be 1.9%.

An important open question about the glass transition is whether there is an underlying thermodynamic transition (see Refs. 3 and 4 and references therein). Usually the highest extrapolated thermodynamic limiting point for the supercooled liquid is the Kauzmann temperature T_K , where the extrapolated entropy of the supercooled liquid becomes equal to the entropy of the crystal. From thermodynamic data available for B₂O₃,²⁰ T_K may be estimated to be 410 K, which is well below the temperature regime of the glass transition with $(T_G - T_K)/T_G = 0.20$. Also the density of the glass at room temperature after cooling at 0.001 K/min, 1.85 g/cm³, is considerably smaller than the density of the crystal, 2.46 g/cm³. Thus the glass formed on a time scale of several weeks is far away from the thermodynamic limiting points based on the comparison with the properties of the crystal. A classification by Angell distinguishes strong and fragile glasses based on the proximity of T_G to T_K , and the curvature of the Arrhenius plot of the viscosity.¹¹ B₂O₃ is a fairly strong glass former according to both criteria. This could be the reason why the delayed response model, which assumes that the glass transition depends only on the kinetics and does not include any thermodynamic limiting points, successfully describes the behavior of the glass, and the relationship between T_G and $\log_{10}(\varphi)$ is linear.

A model which assumes a lower bound for T_G , such as Eq. (4), is probably necessary to describe the kinetics of a fragile glass forming system. Amorphous Pd₄₀Ni₄₀P₁₉Si₁ is a fragile glass with a substantially smaller difference between T_G and T_K with $(T_G - T_K)/T_G = 0.068$,⁴ and a significant curvature of the equilibrium viscosity.²¹ The

higher thermal conductivity of the samples limits temperature lag problems in DSC experiments, so that the experimental result that the relationship between T_G and $\log_{10}(\varphi)$ is nonlinear for this system is probably correct. Currently we are planning similar volume expansion measurements for Pd₄₀Ni₄₀P₁₉Si₁ to verify and extend the results for a fragile glass.

CONCLUSION

The measurement of the volume expansion coefficient gives more accurate kinetic data about the glass transition than differential scanning calorimetry. This technique avoids the problems related to background subtraction, diminishing heat flow at slow cooling and heating rates, and allows a self-consistent temperature lag correction based on the data. The comparison of volumetric and calorimetric data shows that the volume and the enthalpy relax in the same way, pointing to a single microscopic process. The linear relationship between T_G and $\log_{10}(\varphi)$ reflects that B₂O₃ is a strong glass former which has at the point where the supercooled liquid freezes a very open structure. Nonetheless a narrowing of the hysteresis loop at the glass transition was observed which is about 10% for a change of the cooling and heating rate by a decade. Two models were used to analyze the data. Although both models describe the hysteresis of the glass transition adequately, neither predicts the rate dependency correctly nor the narrowing of the transition at smaller rates. The delayed response model, which assumes that the glass transition is a purely kinetic process, works very well for a small range of heating rates. The defect concentration model, which is based on the free volume theory, reproduces the data less well. However, as predicted the parameters found from this model are consistent with viscosity measurements. Similar measurements on other systems, in particular fragile glasses, are needed to extend the systematics found here.

ACKNOWLEDGMENTS

We wish to thank Professor B. Muir for his help with building the dilatometer. This research was supported by the Natural Sciences and Engineering Research Council of Canada and Les fonds pour la formation des chercheurs et l'aide à la recherche de la province de Québec.

¹H. N. Ritland, *J. Am. Ceram. Soc.* **37**, 370 (1954).

²M. A. DeBolt, A. J. Easteal, P. B. Macedo, and C. T. Moynihan, *J. Am. Ceram. Soc.* **59**, 16 (1976).

³L. Boehm, M. D. Ingram, and C. A. Angell, *J. Non-Cryst. Solids* **44**, 305 (1981).

⁴R. Brüning and K. Samwer, *Phys. Rev. B* **46**, 11 318 (1992).

⁵M. Rajeswari and A. K. Raychaudhuri, *Phys. Rev. B* **47**, 3036 (1993).

⁶P. B. Macedo and A. Napolitano, *J. Chem. Phys.* **49**, 1887 (1968).

⁷A. K. Hassan, L. M. Torell, L. Börjesson, and H. Doweidar, *Phys. Rev. B* **45**, 12 797 (1992).

⁸M. Misawa, *J. Non-Cryst. Solids* **122**, 33 (1990).

⁹G. V. McCauley, *Bull. Am. Ceram. Soc.* **14**, 300 (1935).

¹⁰S. M. Rehkson, *Glass Science and Technology*, edited by D. R. Uhlmann and N. J. Kreidl (Academic, London, 1986), Vol. 3, p. 100.

¹¹C. A. Angell, *J. Phys. Chem. Solids* **49**, 863 (1988).

¹²S. Yannacopoulos and S. O. Kasap, *J. Mater. Res.* **5**, 789 (1990).

¹³C. T. Moynihan, A. J. Easteal, M. A. DeBolt, and J. Tucker, *J. Am. Ceram. Soc.* **59**, 12 (1976).

¹⁴A. van den Beukel and J. Sietsma, *Acta Metall. Mater.* **38**, 383 (1990).

¹⁵P. A. Duine, J. Sietsma, and A. van den Beukel, *Acta Metall. Mater.* **40**, 743 (1992).

¹⁶P. Tuinstra, P. A. Duine, and J. Sietsma, *J. Non-Cryst. Solids* **156**, 519 (1993).

¹⁷N. Bekkedahl, *J. Res. Nat. Bur. Stand.* **42**, 145 (1949).

¹⁸P. B. Macedo, W. Capps, and T. A. Litovitz, *J. Chem. Phys.* **44**, 3357 (1966).

¹⁹B. P. Bardes, *Metals Handbook*, 9th ed. (American Society for

Metals, Metals Park, OH, 1980), Vol. 3.

²⁰L. B. Pankratz, *Thermodynamic Properties of Elements and Oxides* (Bul. U.S. Bur. of Mines, Washington, D.C., 1982), Vol. 672.

²¹C. A. Volkert and F. Spaepen, *Mater. Sci. Eng.* **97**, 449 (1988).